Supplementary material to "Multivariate Empirical Mode Decomposition", Proceedings of the Royal Society A, 2010

Naveed ur Rehman and Danilo P. Mandic
Communications and Signal Processing Research Group, Dept of Electrical and Electronic Engineering, Imperial College London, London SW7 2AZ, U.K.
Phone: +44-207-594-6271, Emails: {naveed.rehman07, d.mandic}@ic.ac.uk

Abstract

In this material, we provide additional insight into several aspects of the multivariate empirical mode decomposition (MEMD) algorithm [1]. This includes the generation of low-discrepancy pointset on generalized n-spheres, alignment of common scales within multivariate IMFs, and the possible stoppage criteria for MEMD. The material is supported by simulations on synthetic hexavariate signals and real world EEG data.

I. Sampling based on low discrepancy pointsets

We adopt "low discrepancy" quasi-Monte Carlo Hammersley based sequences for generating multi-dimensional pointsets on an n-sphere; these sequences have proven to show considerable improvement, in terms of error bounds, over standard Monte Carlo methods [2]. It has also been shown that the set of direction vectors generated by the Hammersley sequence yields improved generalised discrepancy estimates as compared to other sampling methods, and hence, are uniformly distributed on a sphere [3]. The original hammersley sequence generates the pointset in the range of $[0, 1)$ and hence, therefore, has to be modified to produce the directional vectors on n-sphere. For a particular case of a 2-sphere (three dimensional sphere), this is achieved by first performing a linear scaling of the sequence to the cylindrical domain $(\phi, t) \in [0, 2\pi) \times [-1, 1]$.

To generate sample points distribution on sphere, the transformation from (ϕ, t) to the unit sphere is then achieved via the following radial projection:

$$(\phi, t) \mapsto (\sqrt{1-t^2}\cos(\phi), \sqrt{1-t^2}\sin(\phi), t)^T \tag{1}$$

To generate the uniform samples on a general n-sphere, we first perform a linear mapping to $(n-1)$ angular coordinates, and then generate the direction vectors based on these coordinates.

For illustration, Figure 1(b) and Figure 2 show, respectively, the pointsets on the surface of a three dimensional sphere (2-sphere) and a four dimensional hypersphere (3-sphere), generated by the low discrepancy Hammersley sequence using the transformations discussed above. Observe that, as desired, the points generated by the low discrepancy method are more uniformly distributed as compared to the standard uniform angular approach (Figure 1(a)). In Figure 2, ideally, the pointset should be plotted on a 3-sphere, however, for visualisation purposes, we can only use three 2-spheres. A comparison of the pointset generated by the proposed Hammersley sequence (shown in Figure 2) with that produced based on the uniform angular sampling method (shown in Figure 1(a) and Figure 3, and used in [4]) clearly illustrates the superiority of the proposed method.

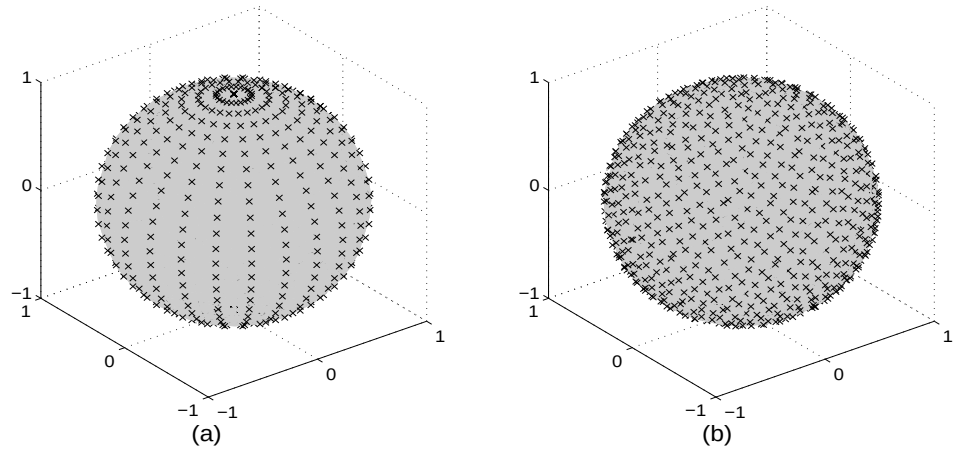

Fig. 1. Direction vectors for taking projections of trivariate signals on a 2-sphere generated by using (a) spherical coordinate system; (b) a low-discrepancy Hammersley sequence. Observe the non-uniformity of the projections in Figure 1(a).

II. The Stoppage Criteria for Multivariate EMD

The standard stoppage criteria in EMD requires IMFs to be designed in such a way that the number of extrema and the zero crossings differ at most by one for S consecutive iterations of the sifting algorithm. The optimal empirical value of S has been observed to be in the range of $2-3$ [5].

Similarly, in [6], an improved stopping criterion is presented, which introduces an evaluation function based on the envelope amplitude, defined as $a(t) = e_{max}(t) - e_{min}(t)$, so that the sifting process is continued till the value of the evaluation function, which is defined as $f(t) = |\frac{m(t)}{a(t)}|$, where m(t) is the local mean signal, is greater or equal to some predefined thresholds. This criterion ensures globally small fluctuations in the mean signal while taking into account overall large excursions in the signal.

In the multivariate EMD algorithm, we can apply both the above criteria to all projections of the input signal and stop the sifting process once the stopping condition is met for all projections. Another possible method may be to stop the sifting process once the stopping criteria is met for any one of the projected signals. However, it has been observed that it may not yield physically meaningful IMFs, especially in cases where large number of projections are considered to compute the local mean.

For the stoppage criteria given in [6], we performed a test to check the dependence of the execution time of the multivariate EMD algorithm on the number of projections used to compute the local mean. The results are plotted in Figure 4, where it can see be seen that there is a linear dependence of the number of projections on the execution time. The test was performed on a synthetic signal with 12 channels (components).

III. Mode alignment using multivariate IMFs

We shall now demonstrate the ability of the proposed extension of EMD to align ‘common scales’ embedded within the multivariate data. To illustrate the mode alignment property of multivariate EMD, a hexavariate signal, with coordinates (U, V, W, X, Y, Z), is synthetically designed such that a single frequency sine wave is made common to all its components, whereas the remaining three tones are made common in UVX, $UVWY$ and $UWXZ$ components; white Gaussian noise is then added to first three components only. The hexavariate signal is first processed via two separate applications of the trivariate EMD algorithm (given in [4], but performed using the quasi Monte Carlo sampling in [1])and the results are shown in Figure 5. It can be seen that the tones separated via the trivariate EMD are not properly aligned in the resulting IMFs. In Figure 6, we show the IMFs obtained by processing the same hexavariate synthetic signal via a single application of the hexavariate EMD. It is evident that the tones are now

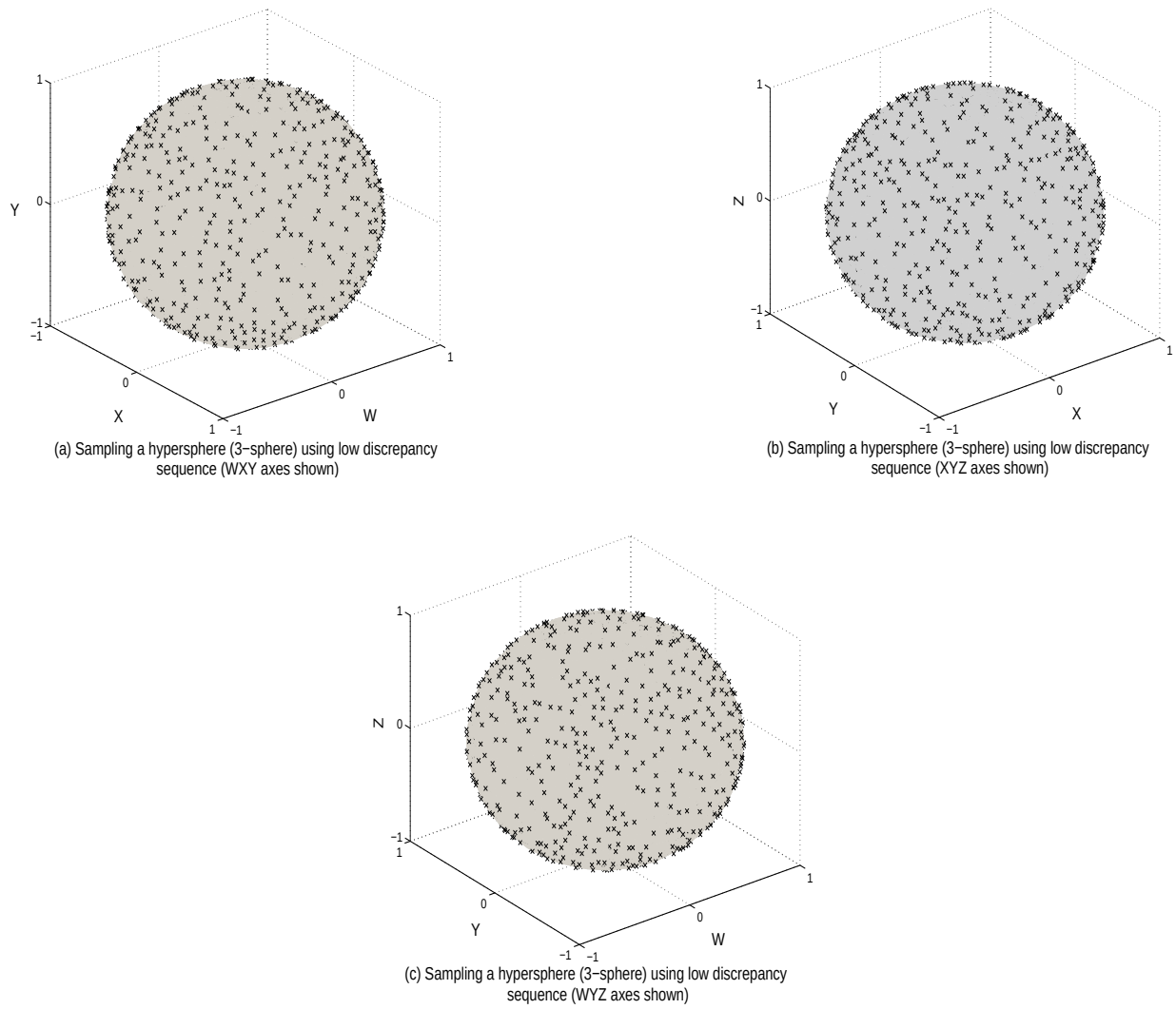

(a) Sampling a hypersphere (3−sphere) using low discrepancy sequence (WXY axes shown)

(b) Sampling a hypersphere (3−sphere) using low discrepancy sequence (XYZ axes shown)

(c) Sampling a hypersphere (3−sphere) using low discrepancy sequence (WYZ axes shown)

Fig. 2. Direction vectors for taking projections of a quaternion signal (with N=4 components) on a unit 3-sphere generated by using a low discrepancy Hammersley sequence. For visualisation purposes, the pointset is plotted on three unit 2-spheres, defined respectively by the WXY, WYZ, and XYZ axes. Observe the enhanced uniformity of the sampling as compared to the method based on uniform angular sampling, shown in Figure 1(a)

properly aligned within the multivaraite IMFs. This mode alignment property is an important requirement for data/sensor fusion applications in the time-frequency domain.

IV. Denoising of real world EEG signals

We now illustrate the power of the proposed method on real world electroencephalography (EEG) signals, with an aim to separate the brain electrical activity from other artefacts such as electrooculography (EOG) and electromyography (EMG). Solution to these problems is an important step for the accurate analysis of the information processing mechanism of the brain and is an active area of research [7] [8] [9]. The data used in these simulations are collected by connecting EEG electrodes to the head channels $Fp1$, $Fp2$, $C3$, $C4$, $F3$, $F4$, $T7$, and $T8$, as described in [10]. Such setting normally prompts subjects to move their eyes often resulting an ocular interference in recorded EEG signal.

The resulting eight channels are then processed via multivariate EMD. Owing to the mode alignment property of the proposed algorithm, the decomposed EEG data is synchronized in multivariate IMFs in such a way that the high frequency neurophysiological signals are separated in lower index IMFs, while

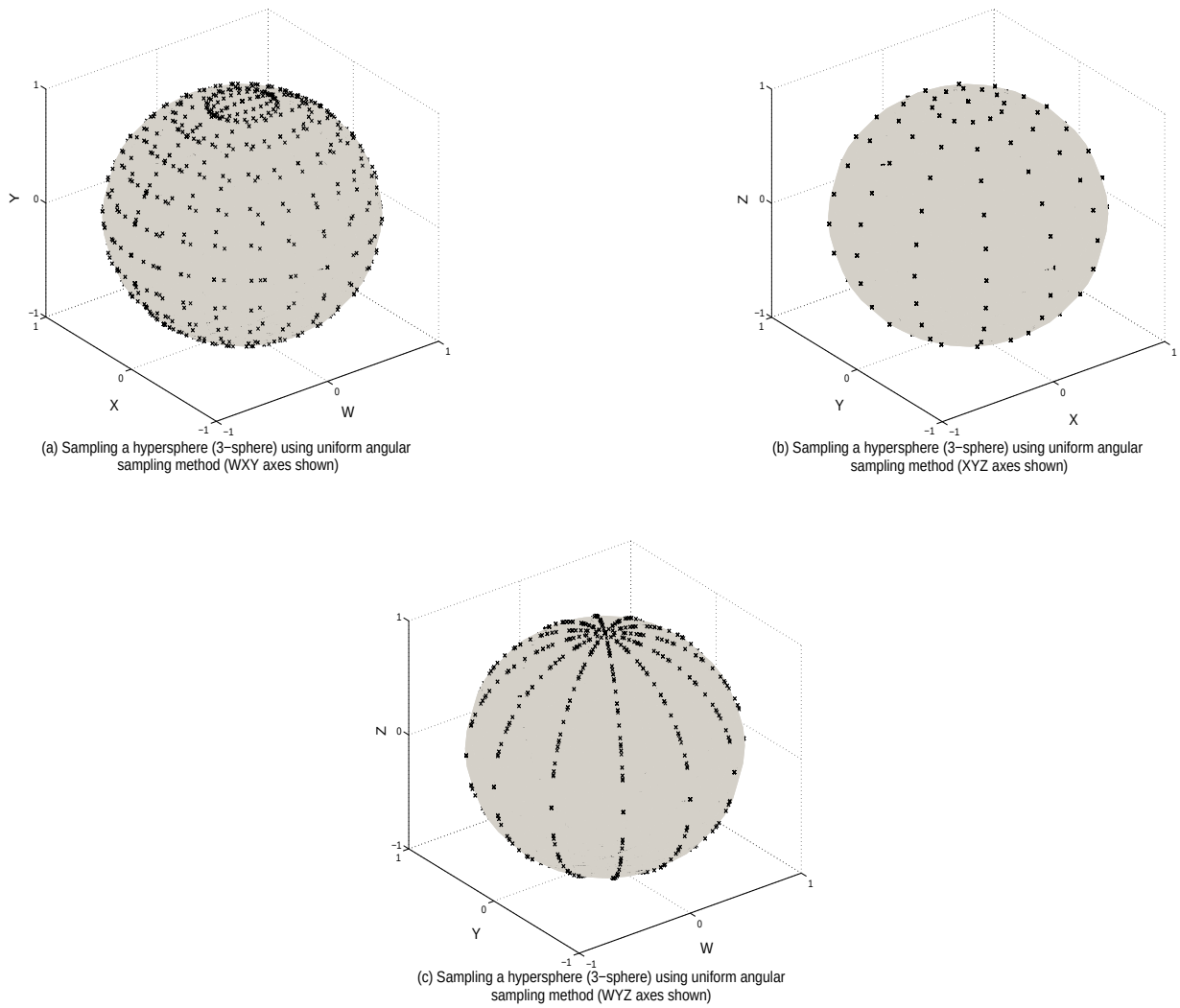

(a) Sampling a hypersphere (3−sphere) using uniform angular sampling method (WXY axes shown)

(b) Sampling a hypersphere (3−sphere) using uniform angular sampling method (XYZ axes shown)

(c) Sampling a hypersphere (3−sphere) using uniform angular sampling method (WYZ axes shown)

Fig. 3. Direction vectors for taking projections of a quaternion signal (with N=4 components) on a unit four dimensional sphere (3-sphere) generated by using a uniform angular sampling method. For visualization purposes, the pointset is plotted on three unit spheres (2-spheres), defined respectively by WXY, XYZ, and WYZ axes.

low frequency electrophysiological signals (EMG and EOG) are contained in high index IMFs. Due to the synchronization property of the proposed method, a simple threshold on IMF index can be used to separate non-EEG related interference from underlying brain activity. The EOG and the clean EEG signal estimated in this way are shown in the middle and right hand column of Figure 7, with original EEG signals shown in the left column. It is important to note that such separation is difficult to achieve by applying univariate EMD on all channels separately as it may result in spectrally uncorrelated components. For instance, in [10], a complex clustering technique is used in the frequency domain (Hilbert transform space) in order to identify spatially correlated modes from univariate EMD decompositions, however, despite to a certain extent, high frequency components are still present in the estimated EOG signal. There were no such problems noticed with our proposed scheme as it effectively aligns the common modes present across multiple channels.

V. Acknowledgements

The EEG data used in Figure 7 were recorded at Advanced Brain Signal Processing Laboratory of RIKEN Brain Science Institute, Japan. We also wish to thank Dr Tomasz Rutkowski for his help in the interpretation of the results in Figure 7.

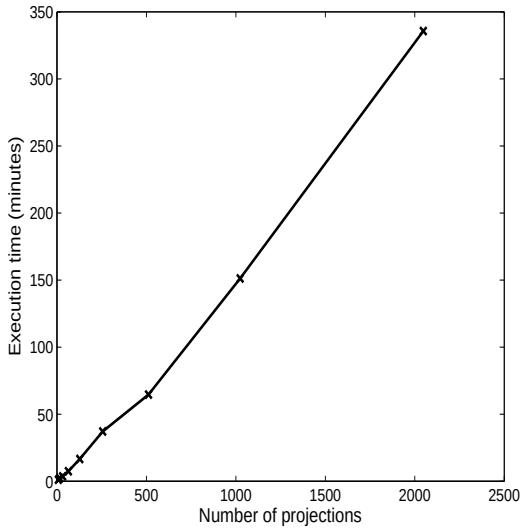

Fig. 4. Dependence of the number of projections on the execution time within the multivariate EMD algorithm.

REFERENCES

[1] N. Rehman and D. P. Mandic, "Multivariate empirical mode decomposition," *Proceedings of the Royal Society A (in print)*, 2010.

[2] H. Niederreiter, *Random number generation and quasi-Monte Carlo methods*, Society for Industrial and Applied Mathematics, 1992.

[3] J. Cui and W. Freeden, "Equidistribution on the sphere," *Siam J. Sci. Comput*, vol. 18, no. 2, pp. 595–609, 1997.

[4] N. Rehman and D. P. Mandic, "Empirical mode decomposition for trivariate signals," *accepted for pubication in proceedings of IEEE Transactions in Signal Processing*, October 2009.

[5] N. E. Huang, M. Wu, S. Long, S. Shen, W. Qu, P. Gloersen, and K. Fan, "A confidence limit for the empirical mode decomposition and Hilbert spectral analysis," *Proceedings of the Royal Society of London A*, vol. 459, pp. 2317–2345, 2003.

[6] G. Rilling, P. Flandrin, and P. Gonalves, "On empirical mode decomposition and its algorithms," in *IEEE-EURASIP Workshop Nonlinear Signal Image Processing (NSIP)*, 2003.

[7] C. A. Joyce, I. F. Gorodnitsky, and M. Kutas, "Automatic removal of eye movement and blink artefacts from eeg data using blind component separation," *Psychophysiology*, vol. 41, no. 2, pp. 313–325, 2004.

[8] D. Looney, L. Li, T. M. Rutkowski, and D. P. Mandic, "Ocular artifacts removal from EEG using EMD," in *Advances in cognitive neurodynamics ICNN 2007 proceedings of the international conference on cognitive neurodynamics*, 2008, pp. 831–834.

[9] T. Gautama, D. P. Mandic, and M. M. Van Hulle, "Indications of nonlinear structures in brain electrical activity," *Phys. Rev. E*, vol. 67, pp. 046204–1–046204–5, 2003.

[10] T. M. Rutkowski, A. Cichocki, T. Tanaka, D. P. Mandic, J. Cao, and A. L. Ralescu, "Multichannel spectral pattern separation-an EEG processing application," *Proceedings of the IEEE International Conference on Acoustics, Speech, Signal Processing*, pp. 373–376, 2009.

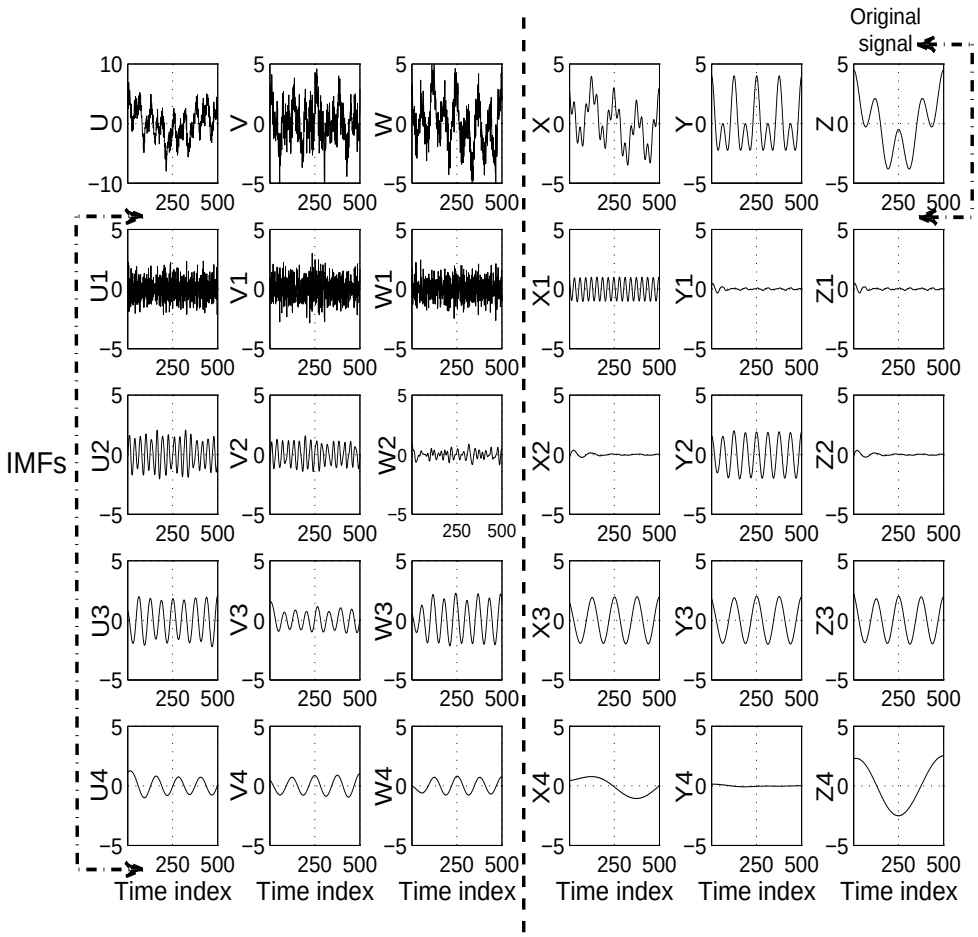

Fig. 5. Decomposition of a two synthetic trivariate signals, with coordinates (U, V, W) and (X, Y, Z), exhibiting multiple frequency modes, via two separate applications of trivariate EMD. Notice that the mode alignment cannot be achieved between components of two separate trivariate inputs as the two signals have been processed separately.

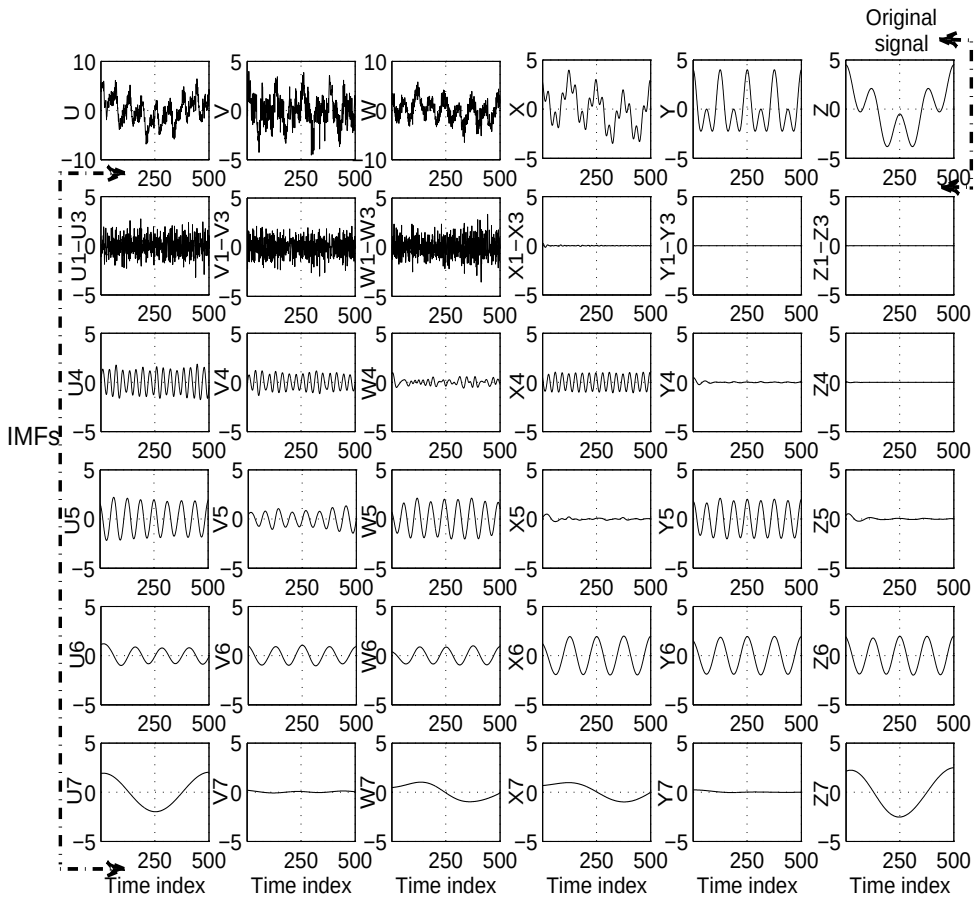

Fig. 6. Decomposition of a synthetic hexavariate signal $(U, V, W, X, Y, Z,)$ exhibiting multiple frequency modes, via the proposed multivariate EMD. Each IMF now carries a single frequency mode, illustrating the alignment of common scales within different components of a hexavaraite signal.

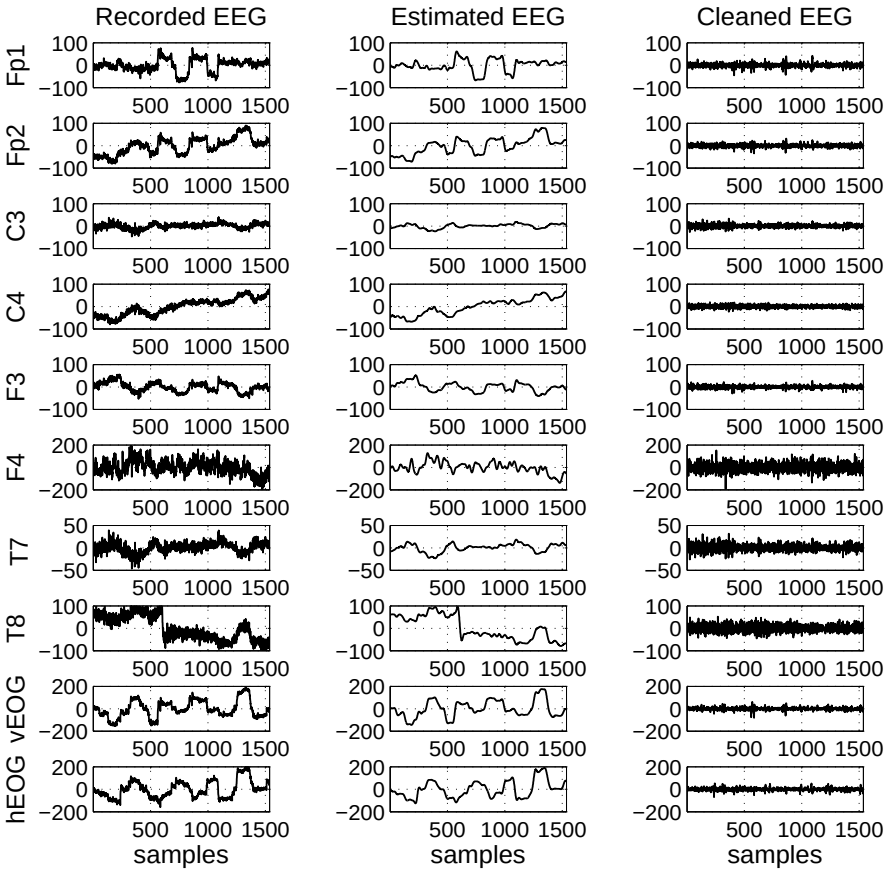

Fig. 7. Illustration of artefact separation from 8 EEG channels ($Fp1$, $Fp2$, $C3$, $C4$, $F3$, $F4$, $C7$, $C8$) and 2 reference EOG channels ($hEOG$ and $vEOG$) using the multivariate EMD algorithm. The estimated muscle activity (artefact) is shown in the middle column, whereas the denoised EEG signal is presented in the right column.